Investigation of various properties of HfO2-TiO2 thin film composites deposited by multi-magnetron sputtering system

Mazur, Michal ; Poniedziaek, A.; Kaczmarek, Danuta; Wojcieszak, Damian; Domaradzki, Jaroslaw; Gibson, D.

Published in:
Applied Surface Science

DOI:
10.1016/j.apsusc.2016.12.129

E-pub ahead of print: 16/12/2016

Document Version
Peer reviewed version

Accepted Manuscript

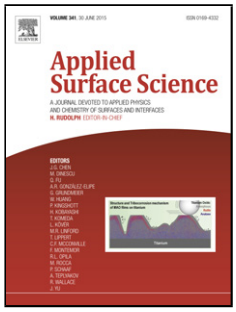

Title: Investigation of various properties of HfO_2-TiO_2 thin film composites deposited by multi-magnetron sputtering system

Author: M. Mazur A. Poniedziałek D. Kaczmarek D. Wojcieszak J. Domaradzki D. Gibson

PII: S0169-4332(16)32857-4
DOI: http://dx.doi.org/doi:10.1016/j.apsusc.2016.12.129
Reference: APSUSC 34676

To appear in: *APSUSC*

Received date: 22-9-2016
Revised date: 14-12-2016
Accepted date: 15-12-2016

Please cite this article as: M.Mazur, A.Poniedziałek, D.Kaczmarek, D.Wojcieszak, J.Domaradzki, D.Gibson, Investigation of various properties of HfO2-TiO2 thin film composites deposited by multi-magnetron sputtering system, Applied Surface Science http://dx.doi.org/10.1016/j.apsusc.2016.12.129

Investigation of various properties of HfO_2-TiO_2 thin film composites deposited by multi-magnetron sputtering system

M. Mazur[1], A. Poniedziałek[1], D. Kaczmarek[1], D. Wojcieszak[1], J. Domaradzki[1], D. Gibson[2]

[1]*Wroclaw University of Technology, Faculty of Microsystem Electronics and Photonics, Janiszewskiego 11/17, 50-372 Wroclaw, Poland*

[2]*Institute of Thin Films, Sensors & Imaging, University of the West of Scotland, Scottish Universities Physics Alliance, High Street, Paisley PA1 2BE, United Kingdom*

e-mail of the corresponding author: agata.poniedzialek@pwr.edu.pl

Highlights

1. HfO_2, mixed HfO_2-TiO_2 with various amount of Ti content and TiO_2 thin films were deposited using magnetron co-sputtering

2. The change of the Ti content in mixed oxide had significant impact on the properties of deposited coatings

3. All deposited thin films were well transparent in visible light range

5. With the increase of Ti content in thin films hardness increased from 4.9 GPa to 13.7 GPa

Abstract

In this work the properties of hafnium dioxide (HfO_2), titanium dioxide (TiO_2) and mixed HfO_2-TiO_2 thin films with various amount of titanium addition, deposited by magnetron sputtering were described. Structural, surface, optical and mechanical properties of deposited coatings were analyzed. Based on X-ray diffraction and Raman scattering measuremets it was observed that there was a significant influence of titanium concentration in mixed TiO_2-HfO_2 thin films on their microstructure. Increase of Ti content in prepared mixed oxides coatings caused, e.g. a decrease of average crystallite size and amorphisation of the coatings. As-deposited hafnia and titania thin films exhibited nanocrystalline structure of monoclinic phase and mixed anatase-rutile phase for HfO_2 and TiO_2 thin films, respectively. Atomic force microscopy investigations showed that the surface of deposited thin films was densely packed, crack-free and composed of visible grains. Surface roughness and the value of water contact angle decreased with the increase of Ti content in mixed oxides. Results of optical studies showed that all deposited thin

films were well transparent in a visible light range. The effect of the change of material composition on the cut-off wavelength, refractive index and packing density was also investigated. Performed measurements of mechanical properties revealed that hardness and Young's elastic modulus of thin films were dependent on material composition. Hardness of thin films increased with an increase of Ti content in thin films, from 4.90 GPa to 13.7 GPa for HfO_2 and TiO_2, respectively. The results of the scratch resistance showed that thin films with proper material composition can be used as protective coatings in optical devices.

Keywords: TiO_2, HfO_2, mixed oxides coatings, microstructure, hardness, scratch resistance, optical and surface properties

1. Introduction

Transition metal oxides, such as hafnium dioxide (HfO_2) and titanium dioxide (TiO_2) have been a subject of intense research in the past few years due to their unique properties. These materials are characterized by a good chemical, thermal and mechanical stability, high reactive index and high dielectric constant [1-4].

HfO_2 (hafnia) thin films find wide range of applications in optical industry [2] due to their relatively wide band gap (Eg~5.5eV), high refractive index (n~2) and high dielectric constant (ε~20) [2,3,5]. These coatings are transparent over a wide spectral range, from the ultraviolet to mid-infrared up to ca. 12 μm with low optical absorption and dispersion [1,2,6-8]. HfO_2 thin films are used in optical coating applications, including interference filters, antireflection coatings and high reflectivity mirrors [1,2,6,7,9]. Depending on the deposition conditions, hafnium dioxide can exist in various polymorphs, i.e. monoclinic, tetragonal and cubic. The monoclinic structure (m-HfO_2) is thermodynamically stable in ambient conditions of temperature and pressure. With the increase of temperature it transforms to tetragonal (t-HfO_2, ≥1722˚C) or cubic (c-HfO_2, >2422˚C) structure [2,4,10,11].

Another transition metal oxide from group IV with wide band gap is TiO_2 (titania). Titanium dioxide has high refractive index (2.25-2.60), dielectric constant (ε~80-110), transparency in visible and near infrared wavelength region. Additionally, it also exhibits high photocatalytic activity [4,8,12-14]. Titanium dioxide can occur in three different polymorphs: anatase, rutile and brookite, however only first two are significant in potential application. Anatase is low-temperature metastable phase and transforms into the highly stable rutile structure above 700˚C [4,13]. Due to its aforementioned properties and crystal structure, titania thin films can be used in various application fields such as optoelectronics, photocatalysis, solar cells, photovoltaics,

self-cleaning and antibacterial coatings [4,13,15]. TiO_2 with anatase phase can be potentially used in self-cleaning, anti-fogging windows or lenses, due to its high photocatalytic activity. In turn, rutile exhibits high refractive index and stability and therefore can be used in anti-reflective coatings [8,13,16].

Hafnia and titania thin films can be prepared by various methods such as chemical vapor deposition, electron beam evaporation, direct current or radio frequency magnetron sputtering, arc deposition, atomic layer deposition, sol-gel method etc. [4,8,13,17,18-20]. Hafnia and titania thin films can be prepared by various methods such as chemical vapor deposition, electron beam evaporation, direct current or radio frequency magnetron sputtering, arc deposition, atomic layer deposition, sol-gel method etc. [4,8,13,17,18-20]. Compared to other techniques, magnetron sputtering method has many advantages such as e.g. high deposition rate, good adhesion, uniformity and suitability for large area deposition (even in the size of several squared meters) [14]. This is a method that is widely applied in the industry for the deposition of various types of coatings – protective, conducting, optical etc. It allows on deposition of single or multilayer coatings. The advantage of sputtering method is also a capability to produce thin oxide films with nanocrystalline structure [21]. It was previously reported that mixed TiO_2-HfO_2 oxide thin films can be prepared by sputtering of ceramic HfO_2 and TiO_2 targets [22], mosaic target with precisely defined amount of Ti and Hf [23] or by co-sputtering of pure metallic targets in Ar:O_2 gas mixture [24-26].

According to the literature [25] addition of TiO_2 to HfO_2 leads to formation of $Hf_{1-x}Ti_xO_2$ phase with a higher dielectric constant than pure HfO_2 while maintaining thermal stability with silicon. Moreover, HfO_2 and TiO_2 mixed oxides exhibit remarkable thermal stability [3,27] that is also confirmed by binary oxide phase diagram [28]. According to the He et al. [29], HfO_2 thin films doped with Ti do not increase oxygen vacancies and cause a decrease of the leakage current in the film, which is desired in the CMOS devices. Jin et al. [3] showed the influence of deposition power on the structure, optical and electrical properties of $HfTiO_x$ thin films. The mixed oxide films were amorphous and well transparent. Moreover, an increase of the value of band gap, refractive index and decrease of extinction coefficient with the rise of deposition power were observed. In turn, Lim et al. [30] showed an effect of TiO_2 addition on the band structure and the quality of microstructure of the HfO_2. Their result showed a decrease of the band gap energy with increasing concentration of TiO_2. In turn, hardness and optical properties of as-deposited and annealed at 800˚C $HfTiO_4$ coatings were studied by Mazur et al. [26]. Thin films prepared by magnetron co-sputtering method had nanocrystalline $HfTiO_4$ structure. The as-deposited films had 3-times higher hardness as-compared to annealed ones (~3 GPa). Moreover, after

annealing, coatings were still well transparent, while the values of refractive and extinction coefficient were slightly higher.

In this paper, mixed hafnia and titania thin films were deposited by reactive magnetron co-sputtering using multitarget stand. The structural, surface, optical and mechanical properties of as-deposited films have been investigated.

2. Experimental details

Five sets of thin films were deposited by reactive magnetron sputtering method, i.e. HfO_2, TiO_2 and three set of mixed HfO_2-TiO_2 oxides with various material composition. During the deposition metallic Hf (99.5%) and Ti (99.99%) targets were co-sputtered for 300 min in oxygen atmosphere with the gas flow 36 sccm. The working pressure in the chamber was equal to $1 \cdot 10^{-2}$ mbar. Magnetrons were independently powered by 2 kW DPS pulsed DC power suppliers with the voltage amplitude up to 1800 V. Mixed oxides were co-sputtered from two magnetrons containing hafnium and titanium targets. Various material composition of deposited thin films was obtained by changing the deposition power in each sputtering process using *pulse width modulation* (*PWM*) method. The power delivered to each magnetron was controlled by the time-width of the pulses, i.e. to increase the content of hafnium in prepared coatings the time-width pulse of magnetron containing Hf target was properly extended. Thickness of prepared TiO_2 and HfO_2 coatings was in the range of 260 – 280 nm, while for mixed oxides films it was 360 – 410 nm. Increase of hafnia content in mixed oxide thin films resulted in increased thickness of prepared coatings. Thin films were deposited on silicon (20×20 mm), fused silica (20×20 mm) and TiAlV (diameter 15 mm) alloy substrates to assess their material composition, structural, optical and mechanical properties. The distance between the targets and the substrates was 160 mm. Thin films were deposited on silicon, fused silica and TiAlV alloy substrates to assess their material composition, structural, optical and mechanical properties.

Material composition of thin films were investigated by FESEM FEI Nova NanoSEM 230 scanning electron microscope (SEM) with 30 kV of acceleration voltage equipped with EDAX Genesis energy dispersive spectrometer. Structural properties were determined based on the results of the X-Ray Diffraction (XRD) method. For the measurements, PANalytical Empyrean PIXel3D powder diffractometer with Cu Kα X-ray (1.5406 Å) was used. The correction for the broadening of the XRD instrument was accounted and the crystallite sizes were calculated using Scherrer's equation [31]. Raman spectra were measured using a Thermo Scientific DXR™ Raman Microscope instrument equipped with a CCD camera detector. The spectra were

recorded in the range from 70 to 1000 cm^{-1} with a resolution of < 1 cm^{-1} and the spot size had a diameter of ca. 1.8 μm. The excitation source was a 455 nm blue laser diode at a power of 8 mW. 10 scans were performed for each sample with the exposure time of 90 s.

Analysis of the surface properties of deposited coatings was performed using Bruker by atomic force microscope (AFM) working in a contact mode [32,33]. For the analysis of the AFM images a WSxM ver.5.0 software was used [34]. Wettability of prepared thin films was assessed by measurements performed with the use of Attension Theta Lite optical tensiometer. Contact angle was assessed using deionized water, ethylene glycol and ethanol. Measurements were performed according to the sessile drop method [35]. The surface free energy of the investigated thin films was determined using geometric and harmonic approaches. In the geometric mean approach, values were determined using Owens and Wendt equations, while in the harmonic are based on Wu equations [36,37].

Optical properties were evaluated based on transmission and reflection measurements carried out in the range of 350-1000 nm, at 30˚ angle of incident light, for S and P polarization, using Aquila nkd-8000 spectrophotometer. Based on obtained results refractive index (n) of prepared coatings was determined. Measurements of as-deposited thin films were completed by evaluation of fundamental absorption edge ($\lambda_{cut\text{-}off}$) and optical band gap energy (Eg). For this purpose the experimental system was consisted of an Ocean Optics QE 65000 spectrophotometer and a coupled deuterium-halogen light source.

The micro-mechanical properties of the thin films, such as hardness and Young's modulus, were measured using the CSM Instrument nanoindenter equipped with Vickers diamond indenter. Hardness and Young's modulus were calculated using the method proposed by Oliver and Pharr [38,39] with Poisson ratio of 0.3. Each data point represents an average of five indentations. A number of measurements were carried out for various depths of nanoindentation. In order to precisely measure the "film-only" properties and minimize the impact of the substrate, a method of nanoindentation measurement approximation was implemented [40-42].

Abrasion resistance of the prepared coatings was investigated using the Summers Optical's Lens Coating Hardness Test Kit. Steel wool test was carried out and consisted of rubbing the surface of prepared thin films for 75 cycles with 0 grade steel wool pad using applied load of 1.0 N. The abrasion resistance test was made for the transparent metal oxide coatings according to the well acknowledged standard [43] and literature reports (e.g. [41,44,45]). Surface of transparent oxide thin films was examined for scratch resistance by optical microscope Olympus BX51 working in reflected light mode. Additionally, three-dimensional images of

coating surface before and after scratch tests were obtained with the aid of TalySurf CCI Lite Taylor Hobson optical profiler.

3. Results and discussion

Five sets of hafnia (HfO_2), titania (TiO_2) and mixed HfO_2-TiO_2 thin films with various amount of titanium addition were prepared using magnetron sputtering method. The titanium content in mixed oxides was estimated to 17, 28 and 45 at. %. Taking into consideration that deposited thin films were sputtered in pure oxygen plasma it can be assumed that they were fully oxidized and stoichiometric. The XRD patterns for deposited thin films are shown in Fig. 1. As-deposited HfO_2 thin film exhibited nanocrystalline structure of monoclinic phase with an average crystallites size of ca. 10.7 nm. Thin films with 17 and 28 at. % of titanium exhibited smaller crystallites, of 6.7 and 7.4 nm, respectively. However, increase of the titanium concentration to 45 at. % in the prepared mixed HfO_2-TiO_2 thin films resulted in broad, amorphous-like pattern without visible peaks. In the case of TiO_2, XRD measurements revealed a trace amount of fine crystallites related to the rutile phase with an average crystallites size of ca. 10.6 nm. XRD measurements of as-deposited HfO_2 thin film, revealed a considerable shift of the diffraction peaks towards lower angle (2θ), which indicates presence of a tensile stress. Negligible tensile stress was also occurred in the thin film that contain 17 at. % of Ti, while for coating with 28 at. % of Ti compressed stress was observed. For TiO_2 tensile stress was again observed.

Raman scattering method was used for further microstructure analysis of deposited thin films. The Raman spectrum of the monoclinic HfO_2 are shown in Fig. 2, which demonstrates resonant Raman peaks. Peaks observed at 133, 147, 257, 267, 321, 500 and 675 cm^{-1} can be assigned to the A_g modes, while peaks found at 167, 242, 334 cm^{-1} corresponds to the B_g modes of monoclinic HfO_2 phase, respectively [46,47]. In Fig. 6 a comparison of Raman spectra of prepared mixed HfO_2-TiO_2 thin films with different amount of Ti is presented. The increase of titanium content in mixed oxides coatings resulted in the weakening and broadening of Raman lines that may testify about less crystallized microstructure and more amorphous character of the coatings. The Raman spectrum for $(Hf_{0.55}Ti_{0.45})Ox$ coating indicates that as-deposited thin film was amorphous since no peaks related to crystalline structure were visible. Such results confirmed measurements carried out with the use of XRD method. In turn, strong and sharp peaks were observed for titanium dioxide thin films, which can indicate that this coating had well crystallized structure. Microstructure properties measurements revealed that the increase

of titanium amount in the mixed TiO_2-HfO_2 thin films resulted in a hindering of crystal growth of deposited thin films. Such amorphisation could be caused by the large mismatch between the unit cell volume of hafnia and titania, which in turn could also cause an incorporation of a large number of lattice imperfections and defects to thin films [48].

Titanium dioxide can occur in three different phases: brookite, anatase and rutile. Brookite has orthorhombic crystal structure and 36 Raman active modes ($9A_{1g}+9B_{1g}+9B_{2g}+9B_{3g}$) can be distinguished for its crystal system [49]. While anatase and rutile are tetragonal and have six and four Raman active modes, respectively. Rutile Raman active modes occur at ca. 143 cm^{-1} (B_{1g}), 447 cm^{-1} (E_g), 612 cm^{-1} (A_{1g}) and 826 cm^{-1} (B_{2g}) [49]. Also a peak at ca. 244 cm^{-1} can occur in the spectrum and it is attributed to the multi-photon process or disorder effects [50]. Anatase has six Raman active modes occur at ca. 515 cm^{-1} (A_{1g}), 400 and 519 cm^{-1} ($2B_{1g}$), 144 cm^{-1}, 197 cm^{-1} and 640 cm^{-1} ($3E_g$) [50]. The peaks in the inset of Fig. 2 of as-deposited titanium dioxide are in good agreement with the mentioned reference values for both, anatase and rutile phases. Therefore, this indicates that deposited thin film had mixed anatase-rutile phase. Strong peak of nanocrystalline anatase was observed at 147 cm^{-1} for the $3E_g$ mode. The modes at 398 cm^{-1} ($2B_{1g}$), 517 cm^{-1} ($2B_{1g}$) and 636 cm^{-1} ($3E_g$) were considerably less intense. The modes at 446 cm^{-1} (E_g), 614 cm^{-1} (A_{1g}) and 821 cm^{-1} (B_{2g}) are characteristic for rutile phase. Raman compound vibration peak at 240 cm^{-1} related to the multi-photon process is considered as a characteristic one for rutile [51]. It is worth emphasizing that XRD studies did not show any peaks related to anatase phase in TiO_2 coating. These observations suggest that Raman scattering method used for structural analysis is very sensitive to crystallinity and microstructure of thin films and revealed new information about a structure of as-deposited TiO_2 coating.

AFM measurements were performed in order to extend the information regarding the surface topography of the as-prepared thin films. The three-dimensional AFM images are shown in Fig. 3a-e. The cross-section topography of the surface (marked by green lines in Fig. 3a-e) of prepared thin films are shown in Fig. 3f. In the case of the HfO_2 thin film, the surface was crack-free, densely packed and composed of visible particles, whose maximum height was ca. 15 nm. The particles diameter after addition of 17 at.% and 28 at.% to the hafnia thin films are similar to the HfO_2 thin films, while their maximum height decreased to the ca. 13 nm and 10 nm for $(Hf_{0.83}Ti_{0.17})Ox$ and $(Hf_{0.72}Ti_{0.28})Ox$ thin films, respectively. Further increase of the Ti amount resulted in a decay of the particles. Surface of $(Hf_{0.55}Ti_{0.45})Ox$ was not composed from particles, had a maximum height of 1.3 nm and was the smoothest as-compared to the rest

thin films. In the case of undoped TiO_2 thin film its surface was the roughest and the maximum height of the particles was equal to ca. 19 nm. The height distribution of as-prepared coatings are presented in Fig. 3a-e as insets in AFM surface images. In all cases results showed a symmetric height distribution of particles in the samples which can testify about good homogeneity of the surface. The calculated root mean square (RMS) surface roughness was found to be equal to ca. 2.6 nm for HfO_2 and gradually decreased with the increase of Ti content in the films to ca. 0.2 nm for $(Hf_{0.55}Ti_{0.45})Ox$ coating. Titanium dioxide thin film had the highest value of RMS equal to ca. 3.4 nm. Surface cross-section (Fig. 3f) confirmed that with the increase of the Ti amount the roughness of thin films decreased, except TiO_2 coating.

The analysis of the surface properties of prepared thin films was completed by measurements of wettability and surface free energy. HfO_2 thin films were hydrophobic due to the water contact angle equal to ca 94.5˚±1.4˚. The hydrophobicity of as-deposited hafnia thin film decreased with an increase of the titanium concentration in thin films (Fig. 4a). The water contact angle was equal to 88.1˚±1.7˚, 75.8˚±2.7˚, 70.6˚±2.2˚ for samples containing 17, 28 and 45 at.% of Ti, respectively. In turn, the value of water contact angle for TiO_2 coating slightly increased as-compared to $(Hf_{0.55}Ti_{0.45})Ox$ and was equal to 74.6˚±1.7˚. Therefore, TiO_2 and mixed TiO_2-HfO_2 thin films were considered as hydrophilic. The same tendency was observed for the values obtained for ethylene glycol measurements. In the case of measurements performed with ethanol, contact angles had the smallest values due to the lowest surface tension of used liquids. Ethanol contact angle for all prepared thin films was similar and in the range from ca. 13° to 19°. The results of geometric and harmonic surface free energy (Fig. 4b), confirmed contact angle measurement results, i.e. with the increase of contact angle value the surface free energy decreased. The contact angle and surface free energy measurements results are summarized in Table 1.

Optical properties of deposited thin films were determined based on transmittance (T_λ) and reflectance (R_λ) measurements obtained for S and P polarization and 30˚ of light incidence. Results of these measurements of prepared thin films are presented in Fig. 5a-e. As-deposited samples were transparent in visible wavelength range with the transmittance of approximately 80% for HfO_2 and HfO_2-TiO_2 mixed coatings. In turn, average transmittance for TiO_2 thin film was equal to ca. 70-75% and the visible interferences had the highest amplitude, which could testify about high refractive index of this coating.

The results of fundamental absorption edge ($\lambda_{cut\text{-}off}$) measurements and the dependence of optical band gap energy (E_g) and $\lambda_{cut\text{-}off}$ on Ti atomic content are compared and presented in Fig. 6. In the case of as-deposited thin films, the cut-off wavelength for undoped HfO_2 was equal to 155 nm, while addition of 17 at. % Ti significantly shifted it towards longer wavelength of 277 nm. Further increase of the titanium to 28 at. % and 45 at. % in the thin films caused an increase of cut-off wavelength to 298 nm and 310 nm, respectively. For the titanium dioxide coating, the $\lambda_{cut\text{-}off}$ is equal to 344 nm. The optical band gap energy was determined from Tauc plots for indirect transitions $(\alpha h\nu)^{1/2}$ in the function of photon energy (eV). For HfO_2 thin film E_g was equal to 6.08 eV. The addition of titanium to undoped hafnia coatings caused significant decrease of the optical band gap energy reaching the values from 3.41 eV to 3.36 eV for $(Hf_{0.83}Ti_{0.17})Ox$ and $(Hf_{0.55}Ti_{0.45})Ox$ thin films, respectively. The lowest value of Eg was obtained for TiO_2 thin film and it was two times lower, as-compared to undoped HfO_2. Fig. 6c also presents dependence of refractive index and packing density on Ti atomic content. For calculation of refractive index (n) dispersion curves the reverse engineering method was used with the aid of SCOUT software. It was found that the values of the refractive index are dependent on the Ti content in the thin films. The refractive index for as-deposited coatings increased from 1.81 to 2.41 for HfO_2 and TiO_2, respectively. Values of n for mixed TiO_2-HfO_2 thin films are in the range from 1.86 for $(Hf_{0.83}Ti_{0.17})Ox$ and $(Hf_{0.72}Ti_{0.28})Ox$ to 1.97 for $(Hf_{0.55}Ti_{0.45})Ox$ thin films.

The packing density (PD) of a film is directly related to its refractive index and it is defined as the ratio of the average film density (ρ_f) and the bulk density (ρ_b) according to the Eq. (3) [48,52]:

$$PD = \rho_f/\rho_b \tag{3}$$

In turn, the correlation between the film refractive index (n) and its packing density can be expressed by the Eq. (4):

$$PD = \frac{\left(n_f{}^2 - 1\right)\cdot\left(n_b{}^2 + 2\right)}{\left(n_f{}^2 + 2\right)\cdot\left(n_b{}^2 - 1\right)} \tag{4}$$

where: n_f – refractive index of the thin films at 550 nm, n_b – refractive index of the bulk materials at 550 nm.

The dependence of n and PD on Ti atomic content showed that the lowest value of the refractive index and packing density was obtained for $(Hf_{0.72}Ti_{0.28})Ox$ thin film, while titania film exhibits the highest n and PD. For HfO_2 and mixed TiO_2-HfO_2 coatings, packing densities were very similar.

Mechanical properties were evaluated by nanoindentation measurements. Material composition affected the hardness and Young's modulus of deposited thin films. Fig. 7a-e shows results of hardness measurements of deposited thin films. The results of nanoindentation have shown that hardness of as-deposited nanocrystalline hafnium dioxide thin film was equal to 4.90 GPa . An increase of Ti content in mixed oxides HfO_2-TiO_2 films caused gradual, but small increase of hardness up to ca. 6 GPa for $Hf_{0.55}Ti_{0.45}Ox$ coating. Moreover, a hardness of titanium dioxide was equal to 13.7 GPa, which was the highest value among all investigated coatings. Due to Lin et al. [53] and Kulikovsky et al. [17], the larger amount of rutile phase in the TiO_2 film, the higher hardness values of the TiO_2 films can be reached. Taking into consideration that as-deposited TiO_2 thin films had in fact mixed anatase-rutile phase, obtained hardness was rather high as-compared to pure anatase (~5.0 GPa) or rutile (~16.0 GPa) [42,54].

Fig. 8. shows dependence of hardness and Young's elastic modulus on Ti atomic content. Elastic modulus of HfO_2 and TiO_2 thin films were equal 139.4 GPa and 126.1 GPa, respectively. The increase of Ti content in hafnia thin films caused a significant decrease of the Young's modulus value. The value of elastic modulus for mixed oxides was almost the same for all coatings and equal to ca. 100.7 - 104.2 GPa.

The H^3/E^2 value provides information on the resistance of materials to plastic deformation of coatings [55,56]. This equation shows that the contact loads needed to induce plasticity are higher in materials with larger values of H^3/E^2, i.e., the likelihood of plastic deformation is reduced in materials with high hardness and low modulus, with H^3/E^2 being the controlling material parameter [55]. The values of the plastic resistance parameter H^3/E^2 for the prepared thin films are included in Table 2. The highest value of H^3/E^2 was equal to 0.162 for the as-deposited TiO_2 thin films, compared to the HfO_2 thin films, which was the lowest and equal to 0.006. The results have shown that an increase of Ti content in mixed HfO_2-TiO_2 oxides films, caused gradual increase of plastic resistance parameter from 0.012 up to ca. 0.017-0.019 for $(Hf_{0.83}Ti_{0.17})Ox$ and $(Hf_{0.55}Ti_{0.45})Ox$ coatings, respectively.

In the case of deposited mixed oxide thin film with possible application in optical or optoelectronic devices their tribological properties are crucial. For this reason investigation of scratch resistance was also carried out. The three-dimensional profiles Fig. 9a-e showed that the surface of all prepared thin films before the scratch test were homogenous with low

roughness of ca. 1 nm. After the steel wool test had been performed, the surface roughness increased in each case. For HfO_2 thin film surface roughness was equal to 0.86 nm before scratch test, while after performing steel wool test it increased to 2 nm. In the case of $(Hf_{0.83}Ti_{0.17})Ox$ and $(Hf_{0.72}Ti_{0.28})Ox$ thin films, the surface roughness increased significantly to 48.6 nm and 62.2 nm, respectively. Moreover, the maximum height of surface topographies increased considerably for $(Hf_{0.83}Ti_{0.17})Ox$ and $(Hf_{0.72}Ti_{0.28})Ox$ coatings. These changes in surface topographies of mixed oxides thin films were caused by deep scratches. Mixed oxide coating with the largest amount of titania had surface roughness equal to 2.2 nm after scratch test. For as-deposited TiO_2 thin films, before and after steel wool test the roughness was very similar and equal to ca. 1 nm. The evaluation of films surface was also performed with an optical microscope and shown at the top of 3D surface profiles in Fig. 9. The results of microscope observations showed negligible traces of scratches, which were visible on the as-deposited HfO_2 and TiO_2 thin films and coating with the highest amount of Ti. However, significant scratches and damages were clearly visible in the images obtained for thin films with at. 17% and 28% of Ti content. These results showed that as-deposited coatings such as HfO_2, TiO_2 and also mixed oxide coating with 45 at.% of Ti can be used as protective coatings in optical devices.

4. Conclusions

In this paper HfO_2, mixed HfO_2-TiO_2 with various amount of Ti content and TiO_2 coatings were deposited using magnetron co-sputtering. The change of the titanium content in mixed oxide thin films resulted in modification of structural, surface, optical and mechanical properties.

In the case of structural properties, XRD studies revealed that except amorphous $(Hf_{0.55}Ti_{0.45})Ox$ thin film, all of the deposited coatings were nanocrystalline. As-deposited HfO_2 and TiO_2 thin films exhibited, monoclinic and rutile phase with the crystallites size of ca. 10.7 nm and 10.6 nm, respectively. Mixed oxides thin films had HfO_2-monoclinic phase with smaller crystallites size, of ca. 6.7 nm and 7.4 nm, for 17 at.% and 28 at.%, respectively. Raman scattering method confirmed growth of the amorphous phase with the increase Ti content. However, the peaks of TiO_2 thin film indicated that deposited thin film had mixed anatase-rutile phase.

The surface of prepared thin films, except $(Hf_{0.55}Ti_{0.45})Ox$ coating, was crack-free, densely packed and composed of visible grains. Root mean square surface roughness results showed that with the increase of Ti amount, the roughness of thin films gradually decreased,

except undoped TiO_2 coating. In the case of contact angle measurements, results showed that the hydrophobicity of undoped HfO_2 film decreased after addition of titanium to as-deposited hafnia thin film.

Optical properties changed significantly with the material composition of each thin film. All deposited coatings were well transparent in the visible wavelength range with the transmittance equal up to 80%. The cut-off wavelength and refractive index increased with the increase Ti content, while the optical band gap decreased. The highest value of packing density was obtained for TiO_2 thin film, while $(Hf_{0.55}Ti_{0.45})Ox$ coating exhibits the lowest value of PD.

Nanoindentation measurements results showed that hardness of prepared thin films increased with an increase of Ti content. The highest value of hardness was obtained for TiO_2 thin film and was over two times higher than for HfO_2 and mixed oxides thin films. The results of plastic resistance parameter H^3/E^2 showed that increase of amount Ti addition, caused gradual increase of plastic resistance parameter from 0.006 to 0.019 for mixed oxides films, while the highest value was equal 0.162 for undoped TiO_2. The scratch resistance results showed that before scratch test all prepared thin films were homogenous with low roughness of ca. 1 nm, while after steel wool test surface roughness increased in each case. The results after steel wool test exhibited that as-deposited coatings HfO_2, TiO_2 and with the highest concentration of Ti can be used as protective coatings.

Acknowledgements

This work was co-financed from the sources given by the Ministry of Science and Higher Education within the Iuventus Plus program (no. IP2014 029473) in the years 2015-2017 and the National Science Centre (NCN) as a research project number DEC-2013/09/B/ST8/00140. Authors would like to thank Prof. Andrzej Sikora from Electrotechnical Institute for AFM measurements and PhD Malgorzata Kalisz from Motor Transport Institute for nanoindentation results.

Literature

[1] M.F. Al-Kuhaili, Optical properties of hafnium oxide thin films and their application in energy-efficient windows, Opt. Mater. 27 (2004) 383-387.

[2] M. Vargas, N.R. Murphy, C.V. Ramana, Structure and optical properties of nanocrystalline hafnium oxide thin films, Opt. Mater. 37 (2014) 621-628.

[3] P. Jin, G. He, M. Liu, D.Q. Xiao, J. Gao, X.F. Chen, R. Ma, J.W. Zhang, M. Zhang, Z.Q. Sun, Y.M. Liu, Deposition power modulated optical and electrical properties of sputtering-derived HfTiOx gate dielectrics, J. Alloy. Compd. 649 (2015) 128-134.

[4] K.H. Choi, N. Duraisamy, N.M. Muhammad, I. Kim, H. Choi, J. Jo, Structural and optical properties of electrohydrodynamically atomized TiO_2 nanostructured thin films, Appl. Phys. A. 107 (2012) 715-722.

[5] T. Tan, Z. Liu, H. Lu, W. Liu, H. Tian, Structure and optical properties of HfO_2 thin films on silicon after rapid thermal annealing, Opt. Mater. 32 (2010) 432-435.

[6] T.J. Bright, J.I. Watjen, Z.M. Zhang, C. Muratore, A.A. Voevodin, Optical properties of HfO_2 thin films deposited by magnetron sputtering: from the visible to the far-infrared, Thin Solid Films 520 (2012) 6793-6802.

[7] S. Jena, R.B. Tokas, J.S. Misal, K.D. Rao, D.V. Udupa, S. Thakur, N.K. Sahoo, Effect of O_2/Ar gas flow ratio on the optical properties and mechanical stress of sputtered HfO_2 thin films, Thin Solid Films 592 (2015) 135-142.

[8] S.S. Lin, C.S. Liao, S.Y. Fan, Effects of substrate temperature on properties of HfO_2, HfO_2:Al and HfO_2:W films, Surf. Coat. Tech. 271 (2015) 269-275.

[9] F.L. Martinez, M. Toledano-Luque, J.J. Gandia, J. Carabe,W. Bohne, J. Rohrich, E. Strub, I. Martil, Optical properties and structure of HfO_2 thin films grown by high pressure reactive sputtering, J. Phys. D: Appl. Phys. 40 (2007) 5256-5265.

[10] M. Vargas, N.R. Murphy, C.V. Ramana, Tailoring the index of refraction of nanocrystalline hafnium oxide thin films, Appl. Phys. Lett. 104 (2014) 101907.

[11] H. Jiang, R.I. Gomez-Abal, P. Rinke, M. Scheffler, Electronic band structure of zirconia and hafnia polymorphs from the *GW* perspective, Phys. Rev. B 81 (2010) 085119.

[12] D.A.H. Hanaor, C.C. Sorrell, Review of the anatase to rutile phase transformation, J. Mater. Sci. 46 (2011) 855-874.

[13] P.B. Nair, V.B. Justinvictor, G.P. Daniel, K. Joy, V. Ramakrishnan, P.V. Thomas, Effect of RF power and sputtering pressure on the structural and optical properties of TiO_2 thin films prepared by RF magnetron sputtering, Appl. Surf. Sci. 257 (2011) 10869-10875.

[14] J.W. Zhang, G. Hea, L. Zhou, H.S. Chen, X.S. Chen, X.F. Chen, B. Deng, J.G. Lv, Z.Q. Sun, Microstructure optimization and optical and interfacial properties

modulation of sputtering-derived HfO_2 thin films by TiO_2 incorporation, J. Alloy. Compd. 611 (2014) 253-259.

[15] S. Banerjee, D.D. Dionysiou, S.C. Pillai, Self-cleaning applications of TiO_2 by photo-induced hydrophilicity and photocatalysis, Appl. Catal. B: Environ. 176-177 (2015) 396-428.

[16] M. Chandra Sekhar, P. Kondaiah, S.V. Jagadeesh Chandra, G. Mohan Rao, S. Uthanna, Effect of substrate bias voltage on the structure, electric and dielectric properties of TiO_2 thin films by DC magnetron sputtering, Appl. Surf. Sci. 258 (2011) 1789-1796.

[17] V. Kulikovsky, R. Ctvrtlik, V. Vorlicek, J. Filip, P. Bohac, L. Jastrabik, Mechanical properties and structure of TiO_2 films deposited on quartz and silicon substrates, Thin Solid Films 542 (2013) 91-99.

[18] S.S. Lin, H.R. Li, The optical properties of hydrophilic Hf-doped HfO_2 nanoceramic films, Ceram. Int. 39 (2013) 7677-7683.

[19] S.S. Lin, C.S. Liao, The hydrophobicity and optical properties of the HfO_2-deposited glass, Ceram. Int. 39 (2013) 353-358.

[20] G. Aygun, A. Cantas, Y. Simsek, R. Turan, Effects of physical growth conditions on the structural and optical properties of sputtered grown thin HfO_2 films, Thin Solid Films 519 (2011) 5820-5825.

[21] B. Deng, G. He, J.G. Lv, X.F. Chen, J.W. Zhang, M. Zhang, Z.Q. Sun, Modulation of the structural and optical properties of sputtering-derived HfO_2 films by deposition power, Opt. Mater. 37 (2014) 245-250.

[22] C. Ye, C. Zhan, J. Zhang, H. Wang, T. Deng, S. Tang, Influence of rapid thermal annealing temperature on structure and electrical properties of high permittivity HfTiO thin film used in MOSFET, Microelectronics Reliability 54 (2014) 388-392.

[23] J. Domaradzki, D. Kaczmarek, E.L. Prociow, A. Borkowska, R. Kudrawiec, J. Misiewicz, D. Schmeisser, G. Beuckert, Characterization of nanocrystalline TiO_2–HfO_2 thin films prepared by low pressure hot target reactive magnetron sputtering, Surf. Coat. Tech. 200 (2006) 6283-6287

[24] J.W. Zhang, G. He, M. Liu, H.S. Chen, Y.M. Liu, Z.Q. Sun, X.S. Chen, Composition dependent interfacial thermal stability, band alignment and electrical properties of $Hf_{1-x}Ti_xO_2$/Si gate stacks, Appl. Surf. Sci. 346 (2015) 489-496.

[25] M.C. Cisneros-Morales, C.R. Aita, Intrinsic metastability of orthorhombic $HfTiO_4$ in thin film hafnia-titania, Appl. Phys. Lett. 98 (2011) 051909.

[26] M. Mazur, D. Wojcieszak, J. Domaradzki, D. Kaczmarek, A. Poniedziałek, P. Domanowski, Investigation of microstructure, micro-mechanical and optical properties of $HfTiO_4$ thin films prepared by magnetron co-sputtering, Mater. Res. Bull. 72 (2015) 116-122.

[27] M.C. Cisneros-Morales, C.R. Aita, Crystallization, metastable phases and demixing in a hafnia-titania nanolaminate annealed at high temperature, J. Vac. Sci. Technol. A 28 (2010).

[28] H. Okamoto, Hf-Ti (Hafnium-Titanium), J. Phase Equilib. 18 (1997) 672.

[29] G. He, Z.Q. Sun, Y.Q. Ma, M.Z. Wu, Y.M. Liu, S.W. Shi, G. Li, X.S. Chen, L.D. Zhang, Z.B. Fang, Composition dependence of interface control and optimization on the performance of an HfTiON gate dielectric metal-oxide-semiconductor capacitor, Semicond. Sci. Tech. 26 (2011) 1-8.

[30] Y.V. Lim, T.I. Wong, S. Wang, Electronic structure and crystallinity of the HfO_2-TiO_2 thin films, Thin Solid Films 518 (2010) 107-110.

[31] H.P. Klug, E.E. Alexander, X-ray diffraction procedures for polycrystalline and amorphous materials, 2nd ed., John Wiley and Sons, New York, 1974.

[32] A. Sikora, Quantitative normal force measurements by means of atomic force microscopy. Towards the accurate and easy spring constant determination , Nanoscience and Nanometrology 2 (2016) 8-29.

[33] A. Sikora, Ł. Bednarz, Dynamic speed control in atomic force microscopy to improve imaging time and quality, Meas. Sci. Technol. 25 (2014) 044005.

[34] I. Horcas, R. Fernandez, J.M. Gomez-Rodriguez, J. Colchero, J. Gomez-Herrero, A.M. Baro, WSxM: a software for scanning probe microscopy and a tool for nanotechnology, Rev. Sci. Instrum. 78 (2007) 013705.

[35] D.Y. Kwok, A.W. Neumann, Contact angle measurement and contact angle interpretation, Adv. Coll. Interfac. 81 (1999) 167-249.

[36] D.K. Owens, R. C. Wendt, Estimation of the surface free energy of polymers, 13 (1969) 1471-1747.

[37] C.D. Volpe, D. Maniglio, M. Brugnara, S. Siboni, M. Morra, The solid surface free energy calculation I. In defence of the multicomponent approach, J. Colloid Interf. Sci. 271 (2004) 434.

[38] ISO/FDIS, Metallic materials-instrumented indentation test for hardness and material parameter, part 1: test method, ISO-International Organization for Standardization, Geneva, Switzerland, 20021-14577.

[39] W.C. Oliver, G.M. Pharr, An improved technique for determining hardness and elastic modulus using load and displacement sensing indentation experiments, J. Mater. Res. 7 (6) (1992) 1564-1583.

[40] Y.G. Jung, B.R. Lawn, M. Martyniuk, H. Huang, X.Z. Hu, Evaluation of elastic modulus and hardness of thin films by nanoindentation, J. Mater. Res. 19 (2004) 3076-3080.

[41] M. Mazur, D. Wojcieszak, D. Kaczmarek, J. Domaradzki, S. Song, D. Gibson, F. Placido, P. Mazur, M. Kalisz, A. Poniedziałek, Functional photocatalytically active and scratch resistantant reflective coating based on TiO_2 and SiO_2, Appl. Surf. Sci. 380 (2016) 165-171.

[42] M. Mazur, J. Morgiel, D. Wojcieszak, D. Kaczmarek, M. Kalisz, Effect of Nd doping on structure and improvement of the properties of TiO_2 thin fims, Surf. Sci. Coat. 270 (2015) 57-65.

[43] ISO/TC 172/SC 7/WG 3 N30 Standard, Spectacle lenses-Test method for abrasion resistance, 1998.

[44] R. Blacker, D. Bohling, M. Coda, M. Kolosey, Development of intrinsically conductive antireflection coatings for the ophthalmic industry, in: 43rdAnnual Technical Conference Proceedings, Denver, Society of Vacuum Coaters. (2000) 212-216.

[45] D. Wojcieszak, A. Poniedziałek, M. Mazur, J. Domaradzki, D. Kaczmarek, J. Dora, Influence of plasma treatment on wettability and scratch resistance of Ag-coated polymer substrates, Mat. Sci. Pol. 34 (2016) 418-426.

[46] A. Ramadoss, S.J. Kim, Synthesis and characterization of HfO_2 nanoparticles by sonochemical approach, J. Alloy. Compd. 544 (2012) 115-119.

[47] R. Wu, B. Zhou, Q. Li, Z.Y. Jiang, W.B. Wang, W.Y. Ma, X.D. Zhang, Elastic and vibrational properties of monoclinic HfO_2 from first-principles study, J. Phys. D Appl. Phys. 45 (2012) 1-8.

[48] M. Mazur, D. Kaczmarek, J. Domaradzki, D. Wojcieszak, A. Poniedziałek, Influence of material composition on structural and optical properties of HfO_2-TiO_2 mixed oxide coatings, Coatings 6 (2016) 1-11.

[49] I.A. Alhomoudi, G. Newaz, Residual stresses and Raman shift relation in anatase TiO_2 thin film, Thin Solid Films 517 (2009) 4372-4378.

[50] R. Danish, F. Ahmed, N. Arshi, M.S. Anwar, B.H. Koo, Facile synthesis of single crystalline rutile TiO_2 nano-rods by solution method, Trans. Nonferrous Metal Soc. 24 (2014) 152-156.

[51] A.H. Mayabadi, V.S. Waman, M.M. Kamble, S.S. Ghosh, B.B. Gabhale, S.R. Rondiya, A.V. Rokade, S.S. Khadtare, V.G. Sathe, H.M. Pathan, S.W. Gosavi, S.R. Jadkar, Evolution of structural and optical properties of rutile TiO_2 thin films synthesized at room temperature by chemical bath deposition method, J. Phys. Chem. Solids 75 (2014) 182-187.

[52] M. Mazur, T. Howind, D. Gibson, D. Kaczmarek, S. Song, D. Wojcieszak, W. Zhu, P. Mazur, J. Domaradzki, F. Placido, Investigation of structural, optical and micromechanical properties of $(Nd_yTi_{1-y})Ox$ thin films deposited by magnetron sputtering, Mater. Design 85 (2015) 377-388.

[53] J. Lin, B. Wang, W.D. Sproul, Y. Ou, I. Dahan, Anatase and rutile TiO_2 films deposited by arc-free deep oscillation magnetron sputtering, J. Phys. D: Appl. Phys. 46 (2013) 084008.

[54] D. Wojcieszak, M. Mazur, J. Indyka, A. Jurkowska, M. Kalisz, P. Domanowski, D. Kaczmarek, J. Domaradzki, Mechanical and structural properties of titanium dioxide deposited by innovative magnetron sputtering proces, Mat. Sci. Pol. 33 (2015) 660-668.

[55] L.C. Chang, C.Y. Chang, Y.I. Chen, Mechanical properties and oxidation resistance of reactively sputtered $Ta_{1-x}Zr_xN_y$ thin films, Surf. Coat. Tech. 280 (2015) 27-36.

[56] T.Y. Tsui, G.M. Pharr, W.C. Oliver, C.S. Bhatia, R.L. White, S. Anders, A. Anders, I.G. Brown, Nanoindentation and nanoscratching of hard carbon coatings for magnetic disks, Mat. Res. Soc. Symp. Proc. 383 (1995) 447-452.

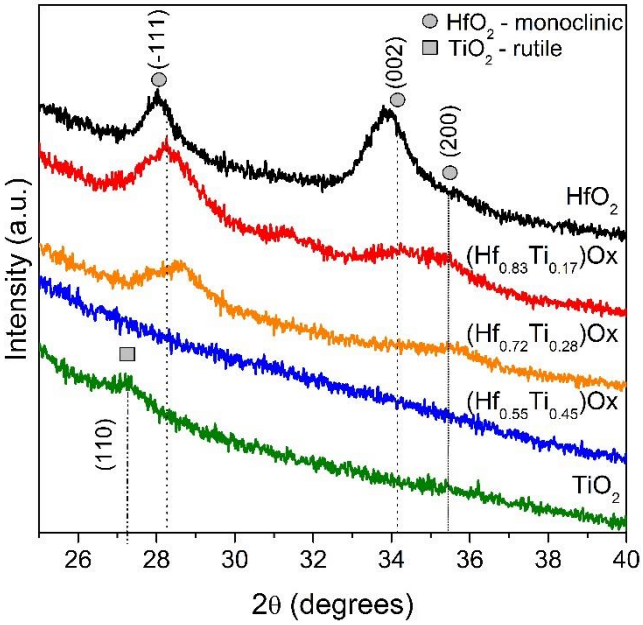

Fig. 1. XRD measurements results of prepared oxide thin films

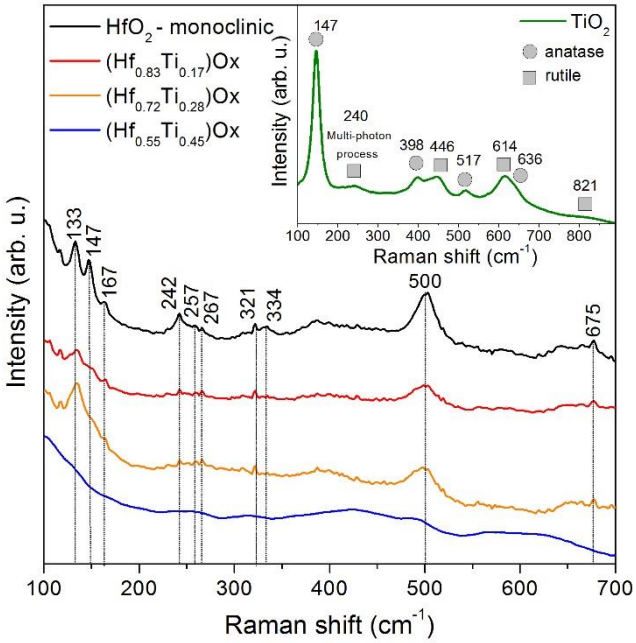

Fig. 2. Raman spectra of the as-prepared HfO_2, TiO_2 and mixed HfO_2-TiO_2 thin films

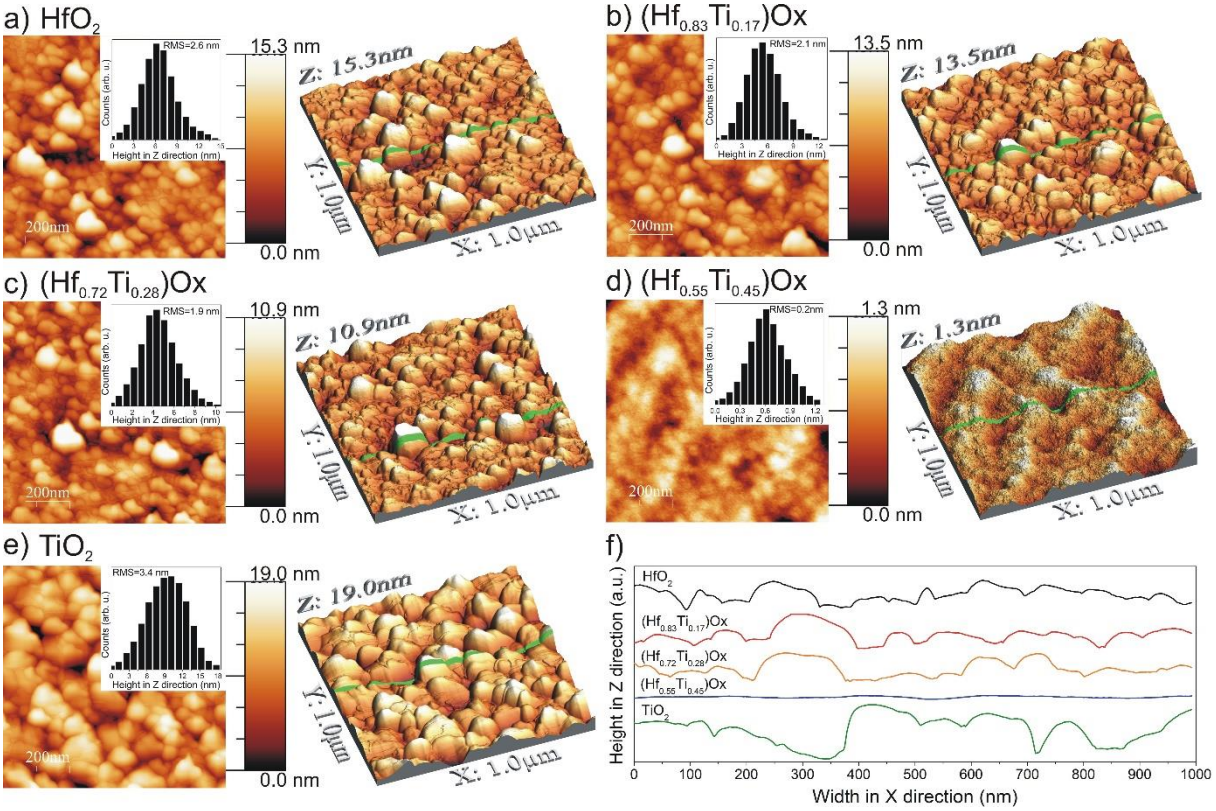

Fig. 3. AFM images with height distribution of particles size in Z direction of: a) HfO_2, b) $(Hf_{0.83}Ti_{0.17})Ox$, c) $(Hf_{0.72}Ti_{0.28})Ox$, d) $(Hf_{0.55}Ti_{0.45})Ox$, e) TiO_2 thin films and f) surface cross-section topography of the as-prepared coatings

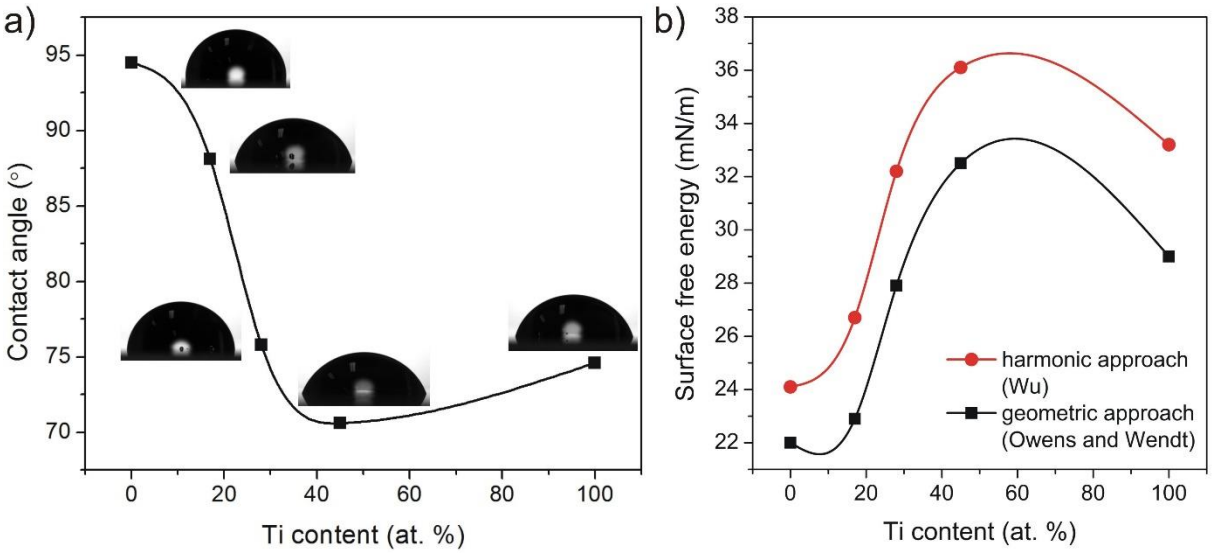

Fig. 4. Dependence of: a) water contact angle and b) surface free energy on Ti atomic content

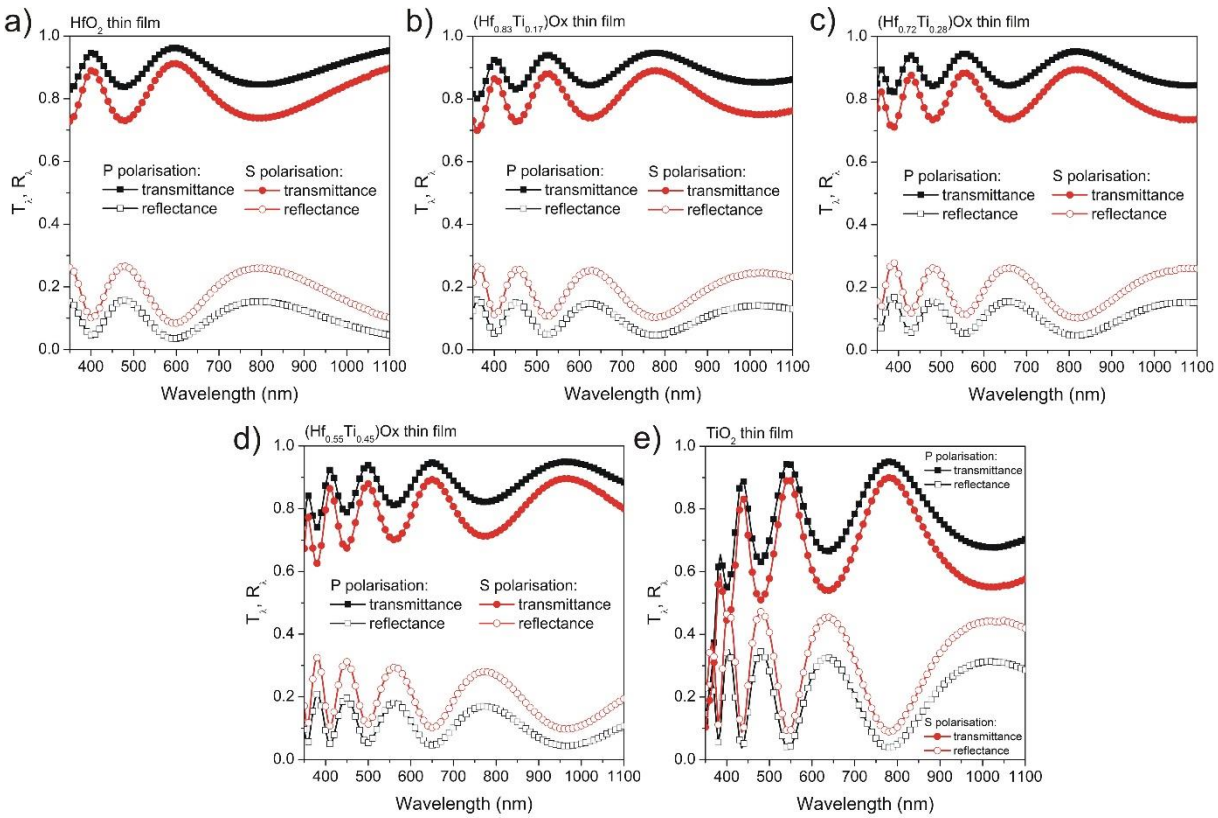

Fig. 5. Transmittance and reflectance spectra taken for S and P polarization of 30º of light incidence for: a) HfO_2, b) $(Hf_{0.83}Ti_{0.17})Ox$, c) $(Hf_{0.72}Ti_{0.28})Ox$, d) $(Hf_{0.55}Ti_{0.45})Ox$ and e) TiO_2 thin films

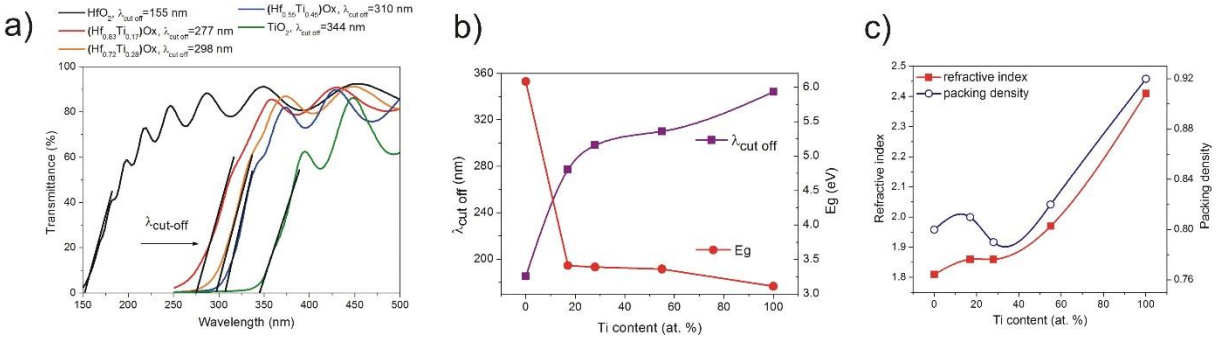

Fig. 6. Results of optical investigations of prepared thin films: a) transmittance spectra in the range from 150 nm to 500 nm for the purpose of fundamental absorption edge ($\lambda_{cut\text{-}off}$) determination and dependence of: b) optical band gap energy and $\lambda_{cut\text{-}off}$; c) refractive index and packing density on titanium content

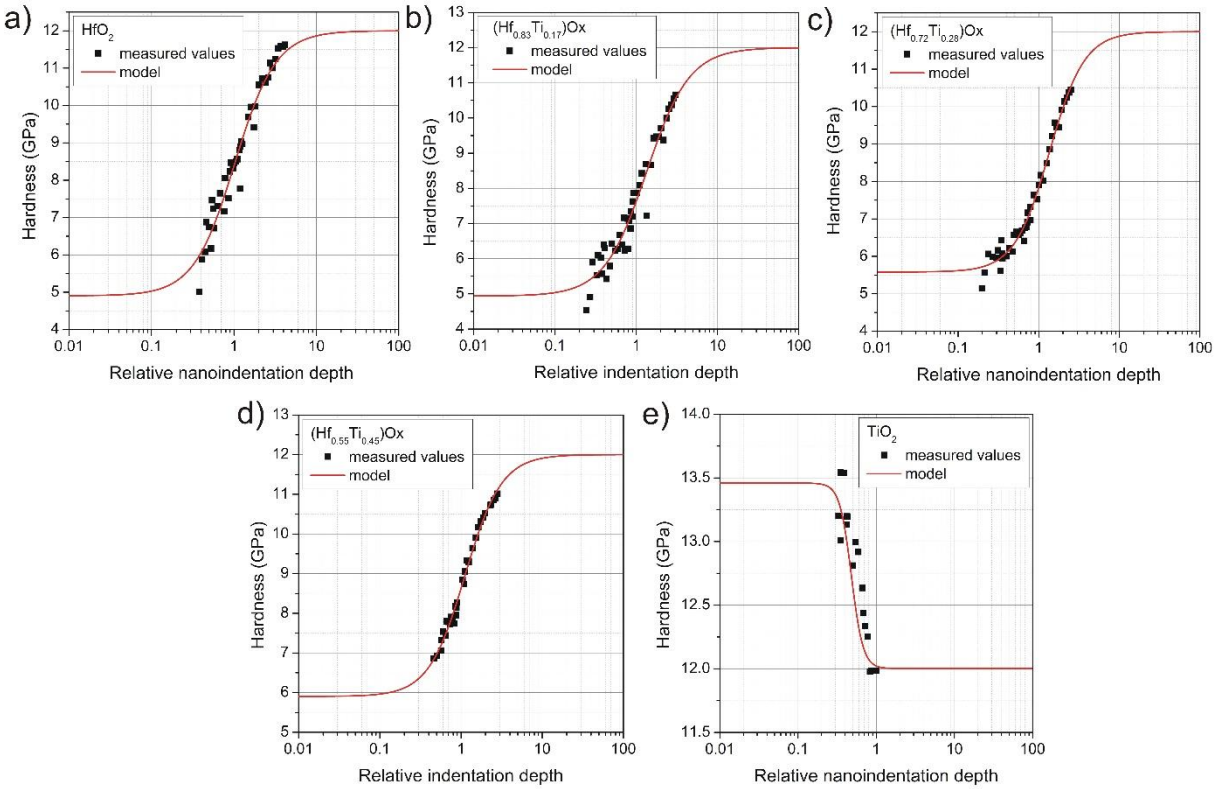

Fig. 7. Results of hardness measurements of: a) HfO_2, b) $(Hf_{0.83}Ti_{0.17})Ox$, c) $(Hf_{0.72}Ti_{0.28})Ox$, d) $(Hf_{0.55}Ti_{0.45})Ox$ and e) TiO_2 thin films

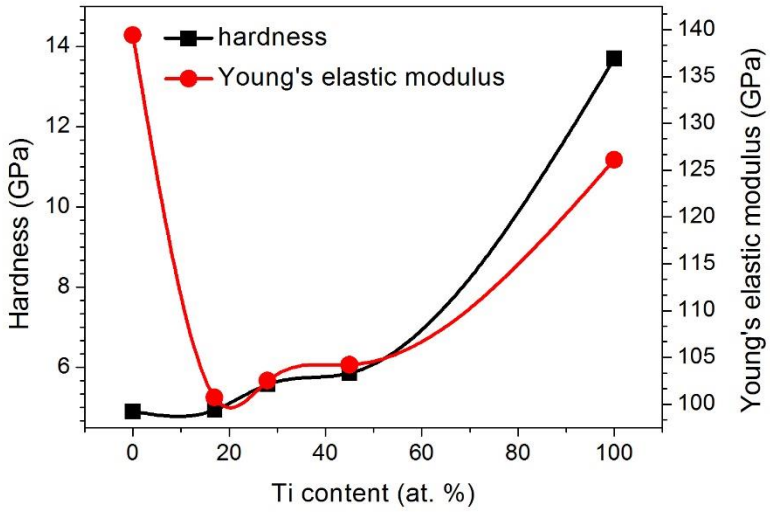

Fig. 8. Dependence of hardness and Young's elastic modulus on Ti atomic content

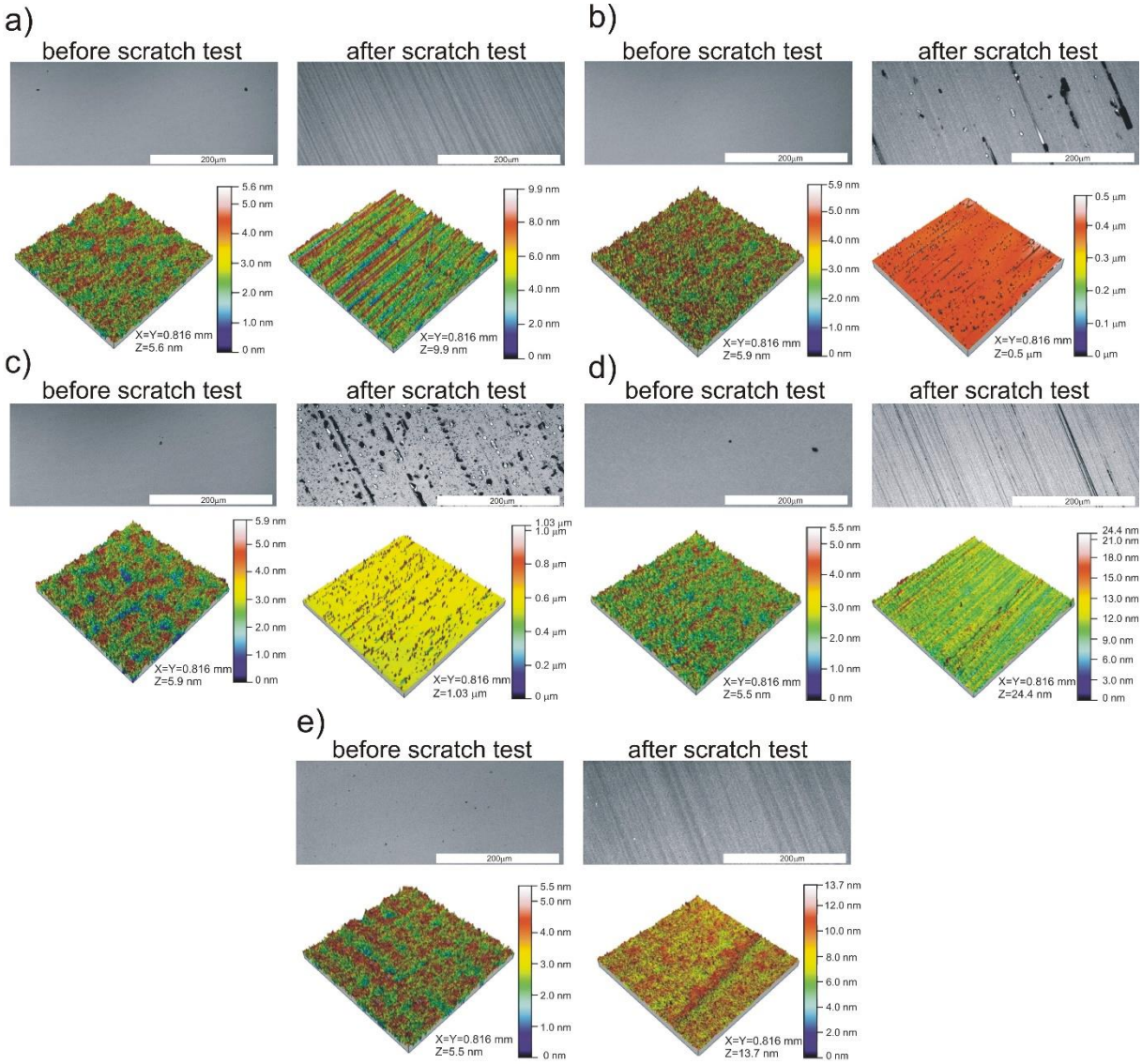

Fig. 9. Results of surface geometry measurements of: a) HfO_2, b) $(Hf_{0.83}Ti_{0.17})Ox$, c) $(Hf_{0.72}Ti_{0.28})Ox$, d) $(Hf_{0.55}Ti_{0.45})Ox$ and e) TiO_2 thin films before and after scratch tests

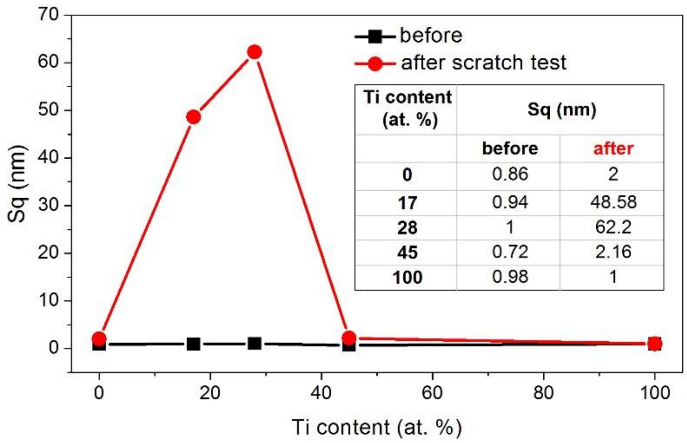

Ti content (at. %)	Sq (nm)	
	before	after
0	0.86	2
17	0.94	48.58
28	1	62.2
45	0.72	2.16
100	0.98	1

Fig. 10. Results of root mean square roughness (Sq) measurements before and after scratch test

Table. 1. Results of critical surface tension and surface free energy investigations prepared oxide thin films

Thin film	Contact angle (˚)			Surface free energy (mN/m)					
				Geometric			Harmonic		
	water	ethylene glycol	ethanol	d	p	t	d	p	t
HfO_2	94.5	71.0	15.6	18.3	3.7	22.0	14.8	9.3	24.1
$(Hf_{0.83}Ti_{0.17})Ox$	88.1	66.0	18.9	15.4	7.5	22.9	13.8	12.9	26.7
$(Hf_{0.72}Ti_{0.28})Ox$	75.8	64.8	14.3	9.5	18.4	27.9	11.4	20.8	32.2
$(Hf_{0.55}Ti_{0.45})Ox$	70.6	55.0	19.4	8.7	23.8	32.5	12.3	23.8	36.1
TiO_2	74.6	61.0	12.9	9.8	19.2	29.0	12.0	21.2	33.2
Designations: d – dispersive component, p – polar component, t – total value of surface free energy									

Table. 2. Results of hardness and Young's elastic modulus of prepared oxide thin films

Thin film	Ti content (at. %)	H (GPa)	E (GPa)	H^3/E^2
HfO_2	0	4.9	139.4	0.006
$(Hf_{0.83}Ti_{0.17})Ox$	17	5.0	100.7	0.012
$(Hf_{0.72}Ti_{0.28})Ox$	28	5.6	102.5	0.017
$(Hf_{0.55}Ti_{0.45})Ox$	45	5.9	104.2	0.019
TiO_2	100	13.7	126.1	0.162